Talanta 86 (2011) 114–120

Contents lists available at SciVerse ScienceDirect

Talanta

journal homepage: www.elsevier.com/locate/talanta

Microwave plasma torch-atomic emission spectrometry for the on-line determination of rare earth elements based on flow injection preconcentration by TiO_2–graphene composite

Junling Zhang[a], Rongmin Cheng[a], Shanshan Tong[a], Xiaowen Gu[a], Xinjun Quan[a], Yunling Liu[a], Qiong Jia[a,*], Jianbo Jia[b,*]

[a] College of Chemistry, Jilin University, Changchun 130022, PR China
[b] State Key Laboratory of Electroanalytical Chemistry, Changchun Institute of Applied Chemistry, Chinese Academy of Sciences, Changchun 130022, PR China

ARTICLE INFO

Article history:
Received 20 June 2011
Received in revised form 11 August 2011
Accepted 13 August 2011
Available online 19 August 2011

Keywords:
TiO_2–graphene composites
Preconcentration
Flow injection
Rare earth elements
Microwave plasma torch-atomic emission spectrometry

ABSTRACT

In this work, we synthesized TiO_2–graphene composite as a novel preconcentration material. It was enclosed in a microcolumn in the on-line flow injection system to adsorb trace light (La), medium (Tb), and heavy (Ho) rare earth elements (REEs) prior to their determinations by microwave plasma torch-atomic emission spectrometry (MPT-AES). Various experimental parameters, such as sample loading time, sample flow rate, sample pH, eluent flow rate, eluent concentration, and interfering ions, were investigated systematically. Under the optimum conditions, the detection limits (three times of standard deviations of blank by 7 reiterations) of La, Tb, and Ho were found to be 2.2, 1.6, and 2.8 $\mu g\,L^{-1}$, with enrichment factors of 17.1, 11.1, and 10.2, respectively. Relative standard deviations for the determination of the target REEs were 3.6%, 1.3%, and 1.4%, respectively ($n=7$). The developed method was validated by the analysis of La, Tb, and Ho in certified reference material (GBW07313, marine sediment) and high purity REE oxide samples.

1. Introduction

As an alternative to inductively coupled plasma-atomic emission spectrometry (ICP-AES), microwave plasma torch-atomic emission spectrometry (MPT-AES) has found its applications in the determination of metal ions with the advantages of high sensitivity and low operation cost [1]. Commonly, direct MPT-AES determination is difficult due to the low sensitivities and matrix effects. Separation and preconcentration steps are often necessary to achieve sensitive and reliable results [2].

Among the various preconcentration methods, adsorption is receiving increasing attention because of the eco-friendly characteristics. Based on the adsorption technique, on-line column preconcentration has been extensively studied because of its advantages of high enrichment factor, high recovery, rapid phase separation, low cost, low consumption of organic solvents, and the ability to combine with different detection instruments. It is well established that the fundamental properties of the adsorption materials are of prime importance because they decide the sensitivity and selectivity of the analytical method. Therefore, many materials possessing good mass transfer property, large surface area, and high adsorption capacity are explored as adsorbents, such as activated carbon [3,4], C18 [5], polymers [6], silica gel [7], metal alkoxide glass [8], ion-imprinted materials [9], and various resins [10–13].

Titanium dioxide (TiO_2), one of the most important transition metal oxides, has been applied in many areas, e.g., gas sensing [14], photocatalysts [15], photoelectrodes [16], and solar energy conversion [17]. Possessing its several advantages including high surface-area, catalysis, safety, and stability, the applications of TiO_2 as adsorbents have also been reported by some authors [18–21]. However, TiO_2 is not selective and suffers from complicated matrices when used for the adsorption of metal ions [18]. To solve this problem, modification of TiO_2 is often required. Carbonaceous materials are one kind of supports for the dispersion of TiO_2 in order to exhibit additional functionalities, such as structure, surface area, activity, and conductivity. Among the carbonaceous materials, carbon nanotubes (CNTs) are most frequently investigated in relation to adsorption studies or the treatment of contaminated water and air [22–26]. Various methods have been reported to introduce TiO_2 onto CNTs, such as mechanical mixing, sol–gel synthesis, electrospinning methods, electrophoretic deposition, and chemical vapor deposition. Sol–gel synthesis is preferred because it may lead to a heterogeneous, non-uniform coating of CNTs by TiO_2, showing

* Corresponding authors. Tel.: +86 431 85095621; fax: +86 431 85095621.
E-mail addresses: jiaqiong@jlu.edu.cn (Q. Jia), jbjia@ciac.jl.cn (J. Jia).

0039-9140/$ – see front matter © 2011 Elsevier B.V. All rights reserved.
doi:10.1016/j.talanta.2011.08.030

bare CNTs surfaces and random aggregation of TiO_2 onto the CNTs surface [23].

Graphene, as an allotrope of elemental carbon, has gained increasing interest since it was discovered [27]. It is a one-atom thick layer of carbon, and the carbon atoms are tightly packed into a two-dimensional honeycomb configuration, both of which can maximize its surface area. Furthermore, its small sizes, high mechanical strength, and excellent electrical conductivities expand the scope toward a wide range of promising applications. To the best of our knowledge, however, studies about the use of graphene as a sorbent material are relatively limited, especially for metal ions [28–30]. In Deng et al.'s work [30], graphenes (GNs) were functionalized with PF_6^- and GNs^{PF6} had high adsorption capacities for Pb(II) and Cd(II). The adsorption processes could reach equilibrium in 40 min and the adsorption isotherms were described well by Langmuir and Freundlich isotherm models.

Based on the properties of TiO_2 and graphene (hereafter abbreviated as GN), it is of great interest to develop TiO_2/GN composites as a new adsorbent, aiming at a combined advantages of enhanced adsorption capacities. Nevertheless, there is no reliable document to estimate that if GN can be a unique sorbent when it is modified with TiO_2. In the present work, TiO_2/GN composites were prepared and used as the adsorption materials for flow injection (FI) on-line microcolumn separation/preconcentration before MPT-AES determinations of rare earth elements (REEs). La, Tb, and Ho were selected as representatives for light, medium, and heavy REEs, respectively. In order to achieve the best analytical performance, several experimental parameters, such as sample loading time, flow rate, pH value, eluent flow rate and concentration, were optimized. Meanwhile, the method was applied to detect La, Tb, and Ho in certified reference material and high purity of REE oxide samples under the optimal conditions.

2. Experimental

2.1. Reagents

High purity La_2O_3 (99.999%), Tb_2O_3 (99.999%), Ho_2O_3 (99.999%), and other REE oxides (>99.95%) were purchased from Changchun Institute of Applied Chemistry, Chinese Academy of Sciences (Changchun, China). Original solutions of the three target metal ions were prepared by dissolving the above oxides with concentrated nitric acid and titrated with a standard solution of EDTA at pH 3.0 using xylenol orange as an indicator. Samples of various concentrations were achieved by stepwise dilution. A certified reference material, GBW07313 (marine sediment), was from National Research Centre for Certified Reference Materials (Beijing, China). Ultrapure water was used throughout. All the reagents used were of analytical grade.

2.2. Apparatus

Ultrapure water was prepared by the Milli-Q SP system (Millipore, Milford, MA, USA). MPT-AES employed for spectrometric measurements was from Jilin University Little Swan Instruments Co. Ltd., China. The operating conditions were listed in Table 1. A PB-10 pH meter (Sartorius Scientific Instruments Co. Ltd., Beijing, China) was used for pH measurements. An HH-6 thermostat water bath cauldron (Guohua Electrical Appliances Co. Ltd., Changzhou, China) and a KSW resistance furnace (Shenyang Energy-saving Enterprise, Shenyang, China) were employed for needed temperatures. Ultrasonic processing was conducted at the aid of a CQ25-12 ultrasonic washer (Xinzhi Biotechnology Research Institute, Shanghai, China).

Table 1
MPT-AES operating conditions.

Parameters	Value
Microwave forward power (W)	80
Carrier gas (Ar) flow rate (L min^{-1})	0.8
Support gas (Ar) flow rate (L min^{-1})	0.6
Sheathing gas (O_2) flow rate (L min^{-1})	1.0
Entrance slit width (μm)	5
CCD pixel elements	2048
Optical resolution (nm)	0.065
Data transfer rate (ms)	13
Integration time (ms)	3–65,000
λ_{max} (nm) for La	333.749
λ_{max} (nm) for Tb	350.917
λ_{max} (nm) for Ho	345.600

FT-IR spectra (4000–400 cm^{-1}) in KBr were recorded using an Affinity-1 FT-IR spectrometer (Shimadzu, Japan). The FIA-3100 flow injection system (Vital Instruments Co. Ltd., Beijing, China) was composed of a peristaltic pump, an eight-channel multifunctional valve, and PTFE tubes (0.8 mm i.d.). A glassy column (50 mm × 3 mm i.d.) used for packing the TiO_2/GN composites contained frits and stopcocks (Beion Medical Technology Co. Ltd., Shanghai, China).

2.3. Procedures

2.3.1. Preparation of TiO_2/GN composites

Sol–gel method was employed to synthesize TiO_2/GN composites. GN sheets were prepared by reduction of graphite oxide (GO), which was gained by the oxidation of graphite powder with Hummers method [31]. TiO_2/GN composite was prepared using tetrabutyl titanate and GN sheets as the starting materials by a typical sol–gel method [32]. Briefly, concentrated H_2SO_4 was added into mixtures of graphite and $NaNO_3$, then $KMnO_4$ was gradually added. The mixture was stirred with a mechanical stir bar for 30 min at 35 °C. Distilled water was added into the mixture, followed by adding 30% H_2O_2. After filtered and washed four times, the mixture was dried at 100 °C to obtain GO. 0.117 g GO was dispersed with 200 mL ethanol and sonicated for 30 min to get GO/EtOH. GO/EtOH was added with $NaBH_4$ and stirred for 17 h, and then the resulting filter cake was dispersed in ethanol to obtain GN/EtOH. 10 mL tetrabutyl titanate was added to GN/EtOH slowly and stirred for 24 h. 5 mL acetic acid solution was introduced, followed by stirring for 6 h and adding 2 mL distilled water. At last, the sol was dried at 80 °C and calcined at 450 °C for 2 h to obtain TiO_2/GN composites.

2.3.2. Preparation of microcolumn

Before use, 20 mL 5% HNO_3 solution and 20 mL deionized water were passed through the microcolumn in sequence at a flow rate of 2.0 mL min^{-1} in order to clean the microcolumn. Accurately weighed amount of TiO_2/GN was packed into the microcolumn by "tap and fill" method. A small portion of glass wool was introduced at both ends and the end caps were fitted. The microcolumn was washed with deionized water, 1.5 mol L^{-1} HNO_3, and finally deionized water to remove the remained HNO_3.

2.3.3. Procedure of preconcentration

Fig. 1 shows the on-line preconcentration and determination of the REEs. A typical procedure is as follows. At the beginning, the sample was drawn through the microcolumn for 1.5 min at a flow rate of 2.0 mL min^{-1}. In the elution step, the injection valve was turned to the elution position to propel 1.5 mol L^{-1} HNO_3 through the microcolumn for eluting the analyte retained on the microcolumn. At last, the eluent solution was introduced into MPT-AES. All the experimental work was carried out in triplicate and the average result was presented.

(a) Load position (b) Injection position

Fig. 1. Schematic diagram for the flow injection procedure.

2.4. Sample preparation

The certified reference material (CRM), GBW07313, was treated as the following procedure. About 100 mg CRM was placed in a 15 mL PFA Savillex vial, and then 2 mL HNO_3, 3 mL HF, and 3 mL $HClO_4$ were added. The sealed vial was heated at 140 °C for 24 h. In order to remove HF, 3 mL HNO_3 was added and evaporated three times. The residue was diluted to 100 mL with ultrapure water and sonicated for 30 min.

REE oxide samples were prepared by dissolving the oxides with concentrated nitric acid and diluted to proper concentrations.

3. Results and discussion

3.1. Characterization of TiO_2/GN composites

FT-IR was employed to characterize GN (a), TiO_2 (b), and TiO_2/GN (c), where GN and TiO_2 were prepared similar to TiO_2/GN (Section 2.3.1) but without the step of adding tetrabutyl titanate or preparing GO, respectively. Results were shown in Fig. 2. In Fig. 2(a), the peak in the range of 3200–3700 cm^{-1} may be ascribed to the residue −OH groups those are not reduced from GO [33]. It is obvious that this peak also appears in Fig. 2(c), i.e., the FT-IR spectrum of TiO_2/GN. After mixing the two components, the FT-IR spectrum of the composite becomes a combination of the absorption bands of GN and TiO_2 [34,35].

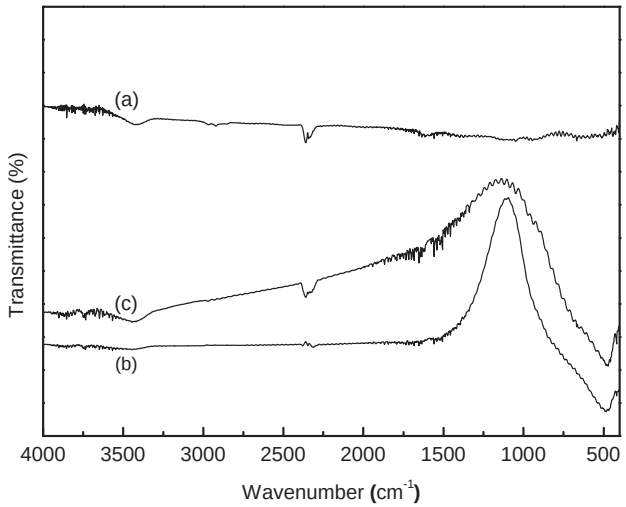

Fig. 2. FT-IR spectra of (a) graphene, (b) TiO_2, and (c) TiO_2/graphene.

3.2. Effect of experimental variables

Variables affecting the emission intensity were investigated and optimized by using the flow injection system combined with the TiO_2/GN microcolumn. The experimental conditions, such as sample loading time, sample flow rate, sample pH, eluent concentration, and eluent flow rate, were examined as follows.

3.2.1. Effect of sample loading time

Fig. 3 shows the effect of sample loading time on the emission intensity. It is obvious that the emission intensity increases with increasing sample loading time (0.5–4.0 min). Although long loading time is a crucial parameter to increase the adsorption, it can reduce analysis frequency which concerns the efficiency of the method. The optimized loading time in the present work was 1.5 min.

3.2.2. Effect of sample flow rate

The sample flow rate is also an important factor to affect the retention of the studied metal ions on the microcolumn containing TiO_2/GN. The experimental results in Fig. 4 state that satisfactory signals of emission can be found when the flow rate is relatively high. Based on an overall consideration of the adsorption capacity and duration of complete analysis, a higher flow rate should be chosen. However, flow rate in higher level needs stronger pressure, which may damage the pipelines and decrease the service life

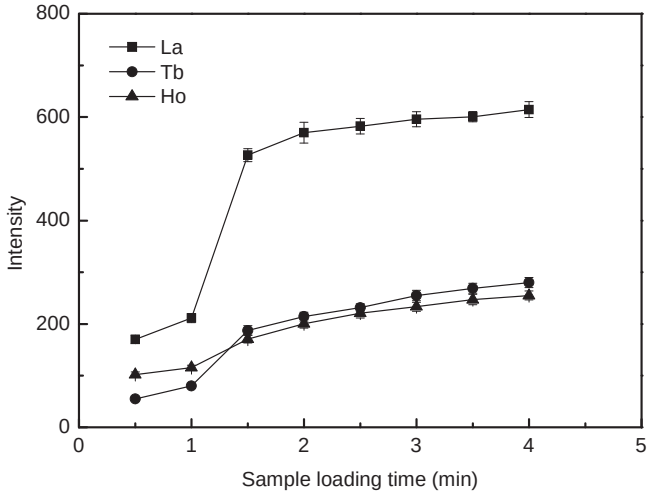

Fig. 3. Effect of sample loading time on emission intensity. Standards: 0.50 μg mL^{-1} for all standards; sample flow rate: 2.0 mL min^{-1}; sample pH: 3.0; eluent: 1.5 mol L^{-1} HNO_3; eluent flow rate: 2.5 mL min^{-1}. The operation conditions of MPT-AES were outlined in Table 1.

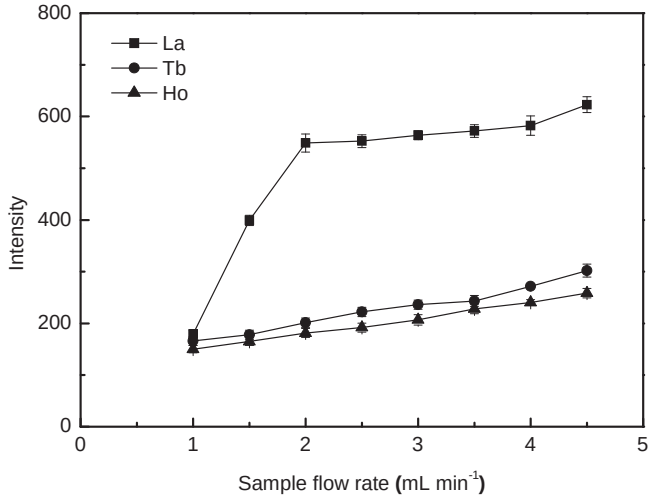

Fig. 4. Effect of sample flow rate on emission intensity. Standards: 0.50 μg mL^{-1} for all standards; sample loading time: 1.5 min; sample pH: 3.0; eluent: 1.5 mol L^{-1} HNO_3; eluent flow rate: 2.5 mL min^{-1}. The operation conditions of MPT-AES were outlined in Table 1.

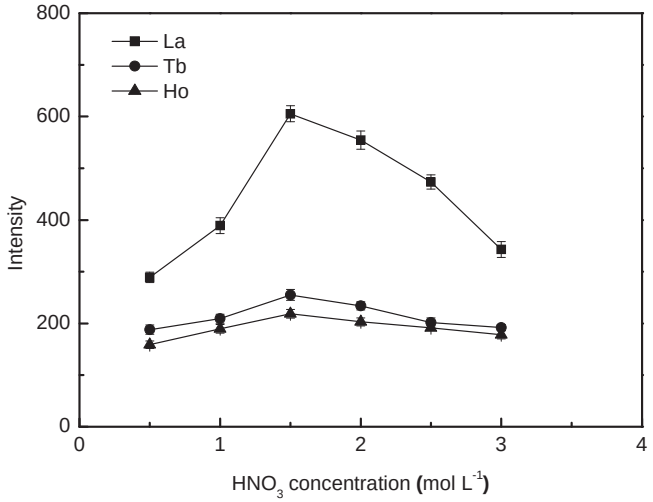

Fig. 6. Effect of HNO_3 concentration on emission intensity. Standards: 0.50 μg mL^{-1} for all standards; sample loading time: 1.5 min; sample flow rate; 2.0 mL min^{-1}; sample pH: 3.0; eluent flow rate: 2.5 mL min^{-1}. The operation conditions of MPT-AES were outlined in Table 1.

of instruments. Moreover, the signal of La increases slightly when the flow rate is greater than 2.0 mL min^{-1}. Therefore, a flow rate of 2.0 mL min^{-1} was selected.

3.2.3. Effect of sample pH

In flow injection on-line systems for metal ions, sample pH is a significant parameter needed to be further studied. Not only the adsorption capacity of TiO_2/GN but also the formation of the REEs complexes depends on the pH value of samples. Traditionally, appropriate control of acidity can avoid hydrolysis process of metal ions, which may facilitate the detection of analytes. To study the influence of the pH value on the adsorption, the sample pH values were adjusted with diluted nitric acid or sodium hydroxide with fixed concentrations of La, Tb, and Ho (0.5 μg mL^{-1}). Such a concentration of REEs leads to negligible hydrolysis even at relative high pH values according to the stability constants of $La(OH)_3$, $Tb(OH)_3$, and $Ho(OH)_3$ [36]. Results of pH dependencies were shown in Fig. 5, which generally indicate that higher sample pH can lead to stronger emission intensity within the range of pH 1.0–7.0. This phenomenon may be attributed to the competition between protons and REEs for the adsorption sites of the sorbent increases at low pH values [22]. Such results are in accordance with some previous reports. For example, Eu(III) sorption on TiO_2 was determined to be strongly pH-dependent [21]. It was suggested that two types of hydroxyl groups exist on the surface of TiO_2, i.e., terminal OH and bridged OH [18]. The adsorption capacity thus increased with increasing pH values. In our previous work [22], the adsorption percentage of Pb(II) with TiO_2/MWCNTs first increased and then changed negligibly as pH increased.

In Fig. 5, the intensity of La increases evidently with increasing pH values. However, the intensity of Tb and Ho does not vary significantly when pH values change. In the present work, REEs solutions were prepared by dissolving the oxides with concentrated nitric acid and diluting stepwise. The pH values of the solutions are about 3.0. Therefore, a sample pH of 3.0 was chosen in the subsequent experiments.

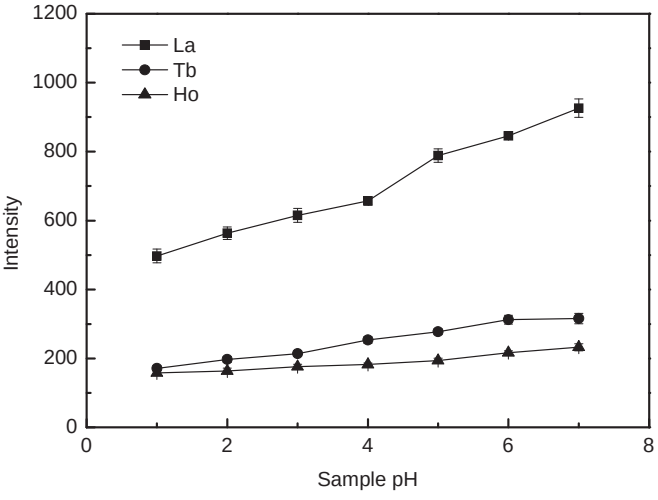

Fig. 5. Effect of sample pH on emission intensity. Standards: 0.50 μg mL^{-1} for all standards; sample loading time: 1.5 min; sample flow rate: 2.0 mL min^{-1}; eluent; 1.5 mol L^{-1} HNO_3; eluent flow rate: 2.5 mL min^{-1}. The operation conditions of MPT-AES were outlined in Table 1.

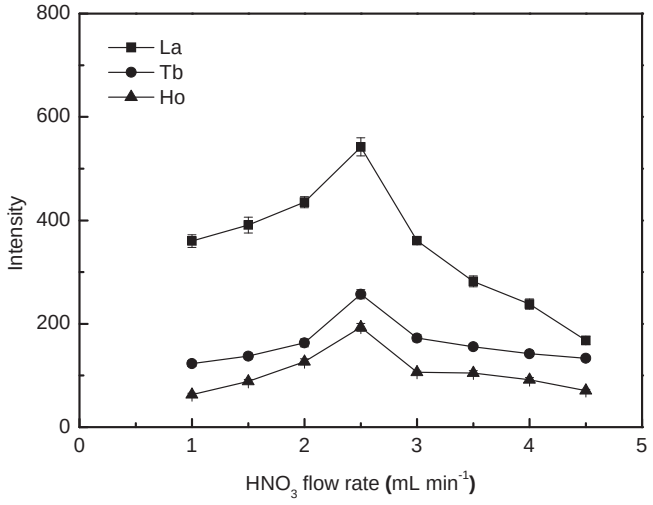

Fig. 7. Effect of HNO_3 flow rate on emission intensity. Standards: 0.50 μg mL^{-1} for all standards; sample loading time: 1.5 min; sample flow rate: 2.0 mL min^{-1}; sample pH: 3.0; eluent: 1.5 mol L^{-1} HNO_3. The operation conditions of MPT-AES were outlined in Table 1.

3.2.4. Effect of eluent concentration

HNO_3 was employed as the eluent in the present work. As one of the most important parameters which has a great effect on the emission intensity, the concentration of HNO_3 was investigated after loading the microcolumn with 0.5 μg mL^{-1} La, Tb, and Ho (Fig. 6). The intensity increases when HNO_3 concentration is up to 1.5 mol L^{-1} while levels off at the concentration greater than 1.5 mol L^{-1}. Too high concentration of HNO_3 may lead to severe corruptions while too low concentration of HNO_3 cannot guarantee sufficient elution of the REEs. In this study, 1.5 mol L^{-1} HNO_3 was selected for the elution of La, Tb, and Ho throughout the experiments.

3.2.5. Effect of eluent flow rate

In order to explore the influence of eluent flow rate on the emission intensity, flow rates in the range of 1.0–4.5 mL min^{-1} were studied by keeping other experimental conditions fixed. Results were shown in Fig. 7, from which it can be concluded that the intensity reaches a maximum value when the flow rate of HNO_3 is 2.5 mL min^{-1}. When the flow rate exceeds 2.5 mL min^{-1}, the intensity decreases because high flow rate generally leads to a loss to contact time between REEs and the eluent. Therefore, 2.5 mL min^{-1} was used for further experiments.

3.3. Interference studies

Interference ions are important problems in the determination of the target analytes in real samples. The effects of several cations and the mutual effects among La, Tb, and Ho were examined under the optimized conditions to evaluate the feasibility of the recommended method. The tolerance limit of interfering ions was defined as the highest amount of foreign ions that produce an error no greater than ±5% in the determination of investigated ions. In these experiments, different amounts of foreign ions were added to a solution containing 0.5 μg mL^{-1} analytes, and then the procedure was implemented to detect the changes of signal. Results were summarized in Table 2, indicating that the proposed method can be used in various samples for the determination of REEs without significant interferences. It is interesting to note that in Duan et al.'s work [1], some easily ionized elements give significant enhancement on analyte signal and that aluminum suppresses the signals considerably. However, similar results were not achieved in the present study, i.e., high tolerance limits of most metal ions were obtained. This should be attributed to the on-line preconcentration procedure with TiO_2/GN microcolumn, which proves itself as an effective strategy for reducing the matrix effects.

Table 2
Effect of diverse ions.

Foreign ions	Tolerance limit (μg mL^{-1})		
	La	Tb	Ho
Al^{3+}	3000	3200	3900
Ca^{2+}	2500	500	3000
Ce^{3+}	450	400	350
Co^{2+}	500	500	400
Cu^{2+}	300	350	350
Dy^{3+}	450	350	550
Ho^{3+}	350	300	–
K^{+}	3800	3500	3500
La^{3+}	–	300	350
Lu^{3+}	400	450	500
Mg^{2+}	1200	800	1000
Na^{+}	2800	3000	3000
Nd^{3+}	400	350	400
Sm^{3+}	500	350	350
Tb^{3+}	350	–	300
Tm^{3+}	400	400	500

3.4. Analytical features

Under the optimized conditions, the linearity of the method was obtained for the studied REEs with high correlation coefficients when the concentrations were ranged from 0.01 to 2.0 μg mL^{-1}.

$$\text{La}: \quad I = 62.012c + 15.174 \quad (R^2 = 0.9975) \tag{1}$$

$$\text{La}: \quad I = 1023.155c - 124.794 \quad (R^2 = 0.9999) \tag{2}$$

$$\text{Tb}: \quad I = 37.405c + 23.043 \quad (R^2 = 0.9913) \tag{3}$$

$$\text{Tb}: \quad I = 414.814c - 120.913 \quad (R^2 = 0.9996) \tag{4}$$

$$\text{Ho}: \quad I = 70.828c + 24.198 \quad (R^2 = 0.9995) \tag{5}$$

$$\text{Ho}: \quad I = 719.342c - 144.429 \quad (R^2 = 0.9991) \tag{6}$$

where I and c express the emission intensity and REEs concentration (μg mL^{-1}), respectively. Eqs. (1), (3), and (5) denote the linear calibration curves without preconcentration and (2), (4), and (6) are those with preconcentration. The enrichment factors (EF) listed in Table 3 were calculated as the ratios between the slopes of the linear

Table 3
Analytical characteristics of the method.

Element	LOD (μg L^{-1})	LOQ (μg L^{-1})	%RSD (n = 7)	EF	Sample throughput (samples h^{-1})
La	2.2	10.4	3.6	17.1	30
Tb	1.6	7.2	1.3	11.1	30
Ho	2.8	11.1	1.4	10.2	30

LOD, limit of detection; LOQ, limit of quantification; EF, enrichment factor.

Table 4
Analytical characteristics of selected on-line adsorption methods for REEs determinations by atomic emission spectrometry.

	Sorbent	Instrument	LOD (μg L^{-1})	Application	Reference
REEs	Silica modified by PAN	ICP-OES	0.011–0.069	Natural water	[5]
REEs	Chitosan-based chelating resin	ICP-AES	0.002–0.25	River water	[11]
La, Ce, Nd, Y	Cinnamene anion exchange resin	MPT-AES	0.78–2.02	High purity REE oxide samples	[12]
Ce, Dy, Eu, La, Yb	Mesoporous titanium dioxide	ICP-OES	0.03–0.35	Environmental samples	[13]
REEs	Flake type chitosan resin	ICP-AES	0.003–0.028	River water	[18]
REEs	DSC-arsenazo on activated carbon	ICP-AES	1.59–9.10	High purity zinc	[37]
REEs	Aminocarboxylic sorbents	ICP-AES	0.1–4.0	Environmental samples	[38]
La	Quinolin-8-ol and Amberlite XAD-7	ICP-AES	0.09	Urine	[39]
REEs	Iron-chlorocomplexes Dowex1X-8	ICP-OES	0.006–0.93	Silicate rocks	[40]
Y	HDEHP adsorbed on a C18 support	ICP-AES	10	Water and biological samples	[41]
La, Tb, Ho	TiO_2/GN	MPT-AES	1.6–2.8	High purity REE oxide samples	Present work

Table 5
Determination results of La, Tb, and Ho in standard reference material GBW07313 and real REE oxide samples (mean ± S.D., $n = 3$).[a]

		La	Tb	Ho
GBW07313	Certified ($\mu g\,g^{-1}$)	67.8 ± 5.7	3.4 ± 0.5	4.3 ± 0.2
	Measured ($\mu g\,g^{-1}$)	65.8 ± 2.7	3.2 ± 0.1	4.4 ± 0.3
CeO_2	Measured ($\mu g\,g^{-1}$)	<LOD	1.06	0.09
	Found ($\mu g\,g^{-1}$)	0.51	1.50	0.53
	Recovery (%)	101.2 ± 2.7	87.3 ± 3.6	88.0 ± 4.2
Nd_2O_3	Measured ($\mu g\,g^{-1}$)	0.04	0.12	0.04
	Found ($\mu g\,g^{-1}$)	0.52	0.62	0.52
	Recovery (%)	96.9 ± 1.9	100.7 ± 5.6	96.0 ± 2.1
Sm_2O_3	Measured ($\mu g\,g^{-1}$)	0.44	1.37	0.28
	Found ($\mu g\,g^{-1}$)	0.89	1.91	0.73
	Recovery (%)	90.3 ± 3.8	108.6 ± 3.5	89.1 ± 3.5
Dy_2O_3	Measured ($\mu g\,g^{-1}$)	0.04	0.68	0.31
	Found ($\mu g\,g^{-1}$)	0.53	1.15	0.81
	Recovery (%)	99.9 ± 0.9	93.5 ± 4.7	100.7 ± 1.2
Tm_2O_3	Measured ($\mu g\,g^{-1}$)	0.71	0.08	0.19
	Found ($\mu g\,g^{-1}$)	1.19	0.55	0.68
	Recovery (%)	96.1 ± 2.6	93.7 ± 3.4	98.4 ± 2.0
Lu_2O_3	Measured ($\mu g\,g^{-1}$)	0.13	0.85	0.04
	Found ($\mu g\,g^{-1}$)	0.58	1.35	0.55
	Recovery (%)	89.9 ± 4.5	99.3 ± 5.1	102.2 ± 2.8

[a] The concentrations of La, Tb, and Ho spiked to REE oxide samples are all 0.5 $\mu g\,g^{-1}$.

calibration curves with and without the on-line preconcentration step. EF values of La, Tb, and Ho were determined as 17.1, 11.1, and 10.2, respectively. A high sample throughput, 30 samples h^{-1}, was also calculated and listed in Table 3.

According to IUPAC recommendations, limits of detection (LODs) are defined as the concentration corresponding to three times the standard deviation of the blanks. Under the optimum conditions, the LODs for La, Tb, and Ho were calculated to be 2.2, 1.6, and 2.8 $\mu g\,L^{-1}$, respectively. Limits of quantification (LOQs) calculated as the blank signal plus ten-times its standard deviations were 10.4, 7.2, and 11.1 $\mu g\,L^{-1}$, respectively. The relative standard deviations (RSD) of our method, obtained for seven determinations of 0.5 $\mu g\,mL^{-1}$ La, Tb, and Ho solutions, were 3.6%, 1.3%, and 1.4%, respectively. All the results were listed in Table 3. As a comparison, some reported on-line adsorption procedures for atomic emission spectrometric determinations of REEs were summarized in Table 4. The present strategy cannot provide the best LOD level. However, it is comparable when considering not only the analytical characteristics but also its advantage of lower capital of operational cost than ICP-AES.

In order to study the stability and potential regeneration of the TiO_2/GN microcolumn, the microcolumn was loaded with the REEs and then the loaded REEs was eluted under the optimized conditions. No obvious decrease in the responses to La, Tb, and Ho solutions was found over 2 months of adsorption–elution operations, implying a feasible multiple use of the microcolumn.

3.5. Validation and applications

Under the optimized conditions, the precision of the developed method was evaluated with the certified reference material (GBW07313) and high purity REE oxide samples. As shown in Table 5, no significant differences were observed between the certified and found values, illustrating that the determined values of the present method coincide well with the certified values.

High purity REE oxide samples were analyzed to verify the applicability of the developed method. The recovery values demonstrated that a sufficient recovery could be achieved (87.3–108.6%). All the figures certified that the developed method could be used for the determination of La, Tb, and Ho in commercial REE oxide samples.

4. Conclusions

A novel sorbent, TiO_2–graphene composite, was synthesized and used for a rapid on-line pretreatment procedure coupled with MPT-AES. All results demonstrated that it can be used for the collection of low concentrations of REEs in the samples, and the ions adsorbed on the composite can be easily eluted with 1.5 $mol\,L^{-1}$ nitric acid solution. In addition, excellent analytical characteristics such as high enrichment factor, sensitivity, accuracy, and good tolerance to interferences of matrix ions, proved a promising application of the method for trace REEs analysis.

Acknowledgement

The project was supported by State Key Laboratory of Inorganic Synthesis and Preparative Chemistry, College of Chemistry, Jilin University (2011).

References

[1] Y.X. Duan, Y.M. Li, X.D. Tian, H.Q. Zhang, Q.H. Jin, Anal. Chim. Acta 295 (1994) 315.
[2] D.M. Ye, H.Q. Zhang, Q.H. Jin, Talanta 43 (1996) 535.
[3] P.L. Mahanta, G. Chakrapani, R. Radhamani, At. Spectrosc. 31 (2010) 21.
[4] N.S. Awwad, H.M.H. Gad, M.I. Ahmad, H.F. Aly, Colloids Surf. B 81 (2010) 593.
[5] N. Bahramifar, Y. Yamini, Anal. Chim. Acta 540 (2005) 325.
[6] Z.H. Wang, X.P. Yan, Z.P. Wang, Z.P. Zhang, L.W. Liu, J. Am. Soc. Mass. Spectrom. 17 (2006) 1258.
[7] N. Zhang, C. Huang, B. Hu, Anal. Sci. 23 (2007) 997.
[8] T. Kajiya, M. Aihara, S. Hirata, Spectrochim. Acta B 59 (2004) 543.
[9] N. Zhang, B. Hu, C.Z. Huang, Anal. Chim. Acta 597 (2007) 12.
[10] Y. Zhu, A. Itoh, T. Umemura, H. Haraguchi, K. Inagaki, K. Chiba, J. Anal. At. Spectrom. 25 (2010) 1253.
[11] R.K. Katarina, M. Oshima, S. Motomizu, Talanta 79 (2009) 1252.
[12] Q. Fu, L. Yang, Q. Wang, Talanta 72 (2007) 1248.
[13] Q. Jia, X. Kong, W. Zhou, L. Bi, Microchem. J. 89 (2008) 82.
[14] E. Palomares, R. Vilar, A. Green, J.R. Durrant, Adv. Funct. Mater. 14 (2004) 111.
[15] D.W. Jing, Y.J. Zhang, L.J. Guo, Chem. Phys. Lett. 415 (2005) 74.
[16] T.N. Murakami, Y. Kijitori, N. Kawashima, T. Miyasaka, J. Photochem. Photobiol. A 164 (2004) 187.
[17] M. Gratzel, Inorg. Chem. 44 (2005) 6841.
[18] C.Z. Huang, Z.C. Jiang, B. Hu, Talanta 73 (2007) 274.
[19] J.M. Pettibone, D.M. Cwiertny, M. Scherer, V.H. Grassian, Langmuir 24 (2008) 6659.
[20] P. Liang, J. Cao, R. Liu, Y. Liu, Microchim. Acta 159 (2007) 35.
[21] Z.J. Guo, S.R. Wang, K.L. Shi, W.S. Wu, Radiochim. Acta 97 (2009) 283.
[22] X.W. Zhao, Q. Jia, N.Z. Song, W.H. Zhou, Y.S. Li, J. Chem. Eng. Data 55 (2010) 4428.

[23] B. Gao, G.Z. Chen, G.L. Puma, Appl. Catal. B: Environ. 89 (2009) 503.
[24] B. Liu, H.C. Zeng, Chem. Mater. 20 (2008) 2711.
[25] C.Y. Kuo, J. Hazard. Mater. 163 (2009) 239.
[26] D. Eder, A.H. Windle, Adv. Mater. 20 (2008) 1787.
[27] K.S. Novoselov, A.K. Geim, S.V. Morozov, D. Jiang, Y. Zhang, S.V. Dubonos, I.V. Grigorieva, A.A. Firsov, Science 306 (2004) 666.
[28] L.B. Hu, X.R. Hu, X.B. Wu, C.L. Du, Y.C. Dai, J.B. Deng, Phys. B 405 (2010) 3337.
[29] K.T. Chan, J.B. Neaton, M.L. Cohen, Phys. Rev. B 77 (2008) 235430.
[30] X.J. Deng, L.L. Lv, H.W. Li, F. Luo, J. Hazard. Mater. 183 (2010) 923.
[31] W.S. Hummers, R.E. Offeman, J. Am. Chem. Soc. 80 (1958) 1339.
[32] X.Y. Zhang, H.P. Li, X.L. Cui, Chin. J. Inorg. Chem. 25 (2009) 1903.
[33] W.S. Ma, J.W. Zhou, S.X. Cheng, J. Chem. Eng. Chin. Univ. 24 (2010) 719.
[34] D.H. Chen, B. Hu, M. He, C.Z. Huang, Microchem. J. 95 (2010) 90.
[35] C. Xu, X. Wang, L.C. Yang, Y.P. Wu, J. Solid State Chem. 182 (2009) 2486.
[36] J.A. Dean, Lange's Handbook of Chemistry, Science Press, 1991, p. 5.
[37] Z.H. Liao, H.N. Ji, L.Z. Li, Z.C. Jiang, Chin J. Anal. Chem. 23 (1995) 1319.
[38] O.N. Grebneva, N.M. Kuzmin, G.I. Tsysin, Y.A. Zolotov, Spectrochim. Acta B 51 (1996) 1417.
[39] O. Vicente, A. Masi, L. Martines, R. Olsina, E. Marchevsky, Anal. Chim. Acta 366 (1998) 201.
[40] R. Lara, R.A. Olsina, E. Marchevsky, J.A. Gasquez, L.D. Martinez, At. Spectrosc. 21 (2000) 172.
[41] Y. Fajardo, E. Gomez, F. Garcias, V. Cerda, M. Casas, Anal. Chim. Acta 539 (2005) 189.